International Journal of Heat and Technology
Vol. 42, No. 2, April, 2024, pp. 373-378
Journal homepage: http://iieta.org/journals/ijht

The Impact of Adhesive Force on Droplet Splash Delay on Surfaces with Nano-Textured Coatings Infused with Lubricant

Narayan P. Sapkal[1*], Nitin P. Sherje[1], Amit S. Chaudhary[1], Kishor B. Waghulde[1], Atul A. Patil[1], Prasanna C. Kattimani[1], Prashant S. Mahapure[1], Prateek D. Malwe[1], Vishal M. Gavande[2]

[1] Department of Mechanical Engineering, Dr. D.Y. Patil Institute of Technology, Savitribai Phule Pune University, Pune 411018, India
[2] Department of Polymer Engineering, Pukyong National University, Busan 48513, Republic of Korea

Corresponding Author Email: narayan.sapkal@dypvp.edu.in

https://doi.org/10.18280/ijht.420202

Received: 11 January 2024
Revised: 9 April 2024
Accepted: 17 April 2024
Available online: 30 April 2024

Keywords:
droplet impact, splash, nano-structures, lubricant infused surface, adhesive force

ABSTRACT

Experimental research is done to determine how the lubricant-infused zinc oxide (ZnO) textures affect the splashing characteristics of droplets. The heat evaporation and photolithography methods are used to create the ZnO-textured surfaces with empty air pockets. When determining critical Weber numbers (We_{cr}) for droplet splashing, the surface properties of ZnO-textured surfaces and the viscosities of the lubricants are taken into account. In relation to lubricant viscosities injected on ZnO textures, the We_{cr} dropped. On lubricant-infused surface's (LIS's) the overall We_{cr} is greater than that of dry ZnO textured surfaces. In comparison to low-viscosity lubricants, the adhesive force has a significant influence in delaying the droplet splash behavior. Results indicate that droplet splashing is caused by an empty air pockets on ZnO surfaces because of the air's existence and the material's weak adherence. While LIS's prevent droplet splashing because of enclosed pockets, excellent adhesion, and the absence of an air layer. Adhesion, therefore, is crucial in minimising droplet splash on surfaces that have been impregnated with lubricant.

1. INTRODUCTION

The super-hydrophobic surfaces (SHSs) have long been studied due to their wide applications such as inkjet printing, pesticide spraying and self-cleaning ability, oil-water separation capacity, resistance to icing, corrosion & fouling, which enables various practical applications in surface engineering, food engineering, photothermal conversion and microfluidic control [1-3]. Particularly, super-hydrophobic surfaces having water contact angle 150° have the excellent water repellency properties [4-6]. This property of SHSs is attributed to the effect of micro/nanoscale roughness of surfaces. An air layer forms between micro/nano scale surfaces and water and thereby reduces the interaction between water and solid surface and water repellency may occur [7-9]. Here capillary pressure prohibits the intrusion of water into the micro/nano textures [10]. Superhydrophobic surfaces are used in droplet-based micro-fluidic systems because their water repellency property allows for the manipulation of water droplet behavior [11, 12]. Though, it's a difficult task to hold a water drop on such superhydrophobic surfaces due to easily roll off from the surface. This issue can be solved by adopting sticky super-hydrophobic surfaces having adhesion and water repellency properties [13-17]. To analyze the adhesion properties of SHSs the droplet splashing dynamics is investigated [18], where droplet splash occurs on SHSs due to the presence of an air layer beneath the drop [19, 20]. Hence, an understanding of droplets impact on SHS is necessary for industrial applications. Based on the surface and drop impact characteristics, the droplet may spread, retract, deposit or bounce. At very high impact velocity and Weber number (We = ratio between kinetic energy and surface energy) droplet splash occur into several satellite droplets [21]. Droplet splashing occurs in two different forms: prompt splashing and corona splashing. Though the droplet splashing dynamics have been studied on various surfaces [22-27], the role of adhesive force in droplet splashing dynamics on lubricant infused surfaces is not yet studied extensively.

Despite the SHS's inherent qualities, drop impact conditions can cause the super-hydrophobicity to fail [28]. Hydrophobic nanostructured surfaces infused with low-surface-tension lubricant oil, on the other hand, can get around these restrictions while still keeping their non-wetting properties. [29, 30]. Here, the non-wetting characteristics of oil-infused surfaces are explained by the fact that the lubricating oil is held in place by the nanowires' surface roughness, and the atomically smooth liquid interface reduces the pinning of the water drop's contact lines, resulting in a low-contact-angle hysteresis. Additionally, the surface is resistant to external pressure and undesirable surface damage due to the lubricating oil's fluidity [29]. It is crucial to understand how lubricant oil surface structure and physical characteristics impact nanostructured lubricant-infused surfaces (LISs). This led to the induction of diverse water drop spreading dynamics on soft

polymer surfaces [31-34]. Due to the liquid nature of the surface, we can anticipate that the water impact dynamics on LISs would differ from those of hard solid surfaces. In the present study, we created open air pocketed zinc oxide (ZnO) nanostructures and chemically treated the surfaces to make them hydrophobic using a low-energy self-assembled monolayer. The effect of oil viscosity and surface condition on splashing is then clarified by fabricating ZnO structured surfaces both with and without the lubricant of varied viscosities. It has been proven that superhydrophobic ZnO surfaces with lubricant infusions control droplet splashing more effectively than superhydrophobic ZnO surfaces with empty air pockets. This phenomenon could be the result of capillary forces pulling water droplets toward the surface from enclosed air pockets.

We are committed to investigating the droplet splashing phenomenon while taking adhesive force and lubricating oil viscosity into account. A high-speed camera is used to visualize droplet splashing phenomena. Thus, at varied LIS surface wetting conditions, the critical Weber numbers (We_{cr} values) of droplet splashing are derived, such as ZnO structured surface with and without lubricant oil. Based on experimental data, we examine the kinetics of droplet splashing on ZnO-structured surfaces both with and without lubricants.

2. SURFACE PREPARATIONS AND EXPERIMENTS

2.1 Surface preparations

To examine the slippery effects on the droplet impact dynamics, we produced a few lubricant-infused surfaces with similar geometrical morphologies but varying lubricant oil viscosities. We bought zinc powder (for evaporation, 99.998%), zinc nitrate hexahydrate (Zn(NO3)26H2O, 98%), and ammonium hydroxide (28 wt% NH3 in water, 99.99%) from Aldrich. A photoresist (AZ5214, AZ electronic materials) and a developer (AZ500MIF, AZ electronic materials) were used to pattern the substrate. Thermal evaporation was used to deposit a layer of zinc oxide onto a silicon substrate. You can use this straightforward evaporation technique on a variety of substrates. The zinc metal layer was between 200 and 250 nm thick. In order to make 20 mM solutions, a calculated quantity of zinc nitrate hexahydrate was dissolved in 200 mL of de-ionized water. To change the pH of the growth fluid, ammonia water (NH4OH) (28 weight percent NH3 in water, 99.99%) was successively added. Depending on the proportion of zinc salt and desired pH, 7.5 mL of ammonia water was added. A Teflon-capped glass bottle containing the growth fluid was used to suspend the Zn/Si substrate upside down during the hydrothermal growth of ZnO nanorods. The chosen growing temperature was 60°C, and the normal development period was 6 hours. The substrate was taken out of the solution after growth, washed with de-ionized water, and dried. The substrate was patterned using the standard photolithography procedure. At a speed of 3000 rpm, a photoresist was spin-coated onto a substrate for 60 seconds. The substrate went through a series of steps including baking, UV exposure of 360 nm precise time of 15 minutes, and development, washing, and drying. A ZnO nanorod array on a patterned substrate was selectively grown using the aforementioned solution technique. A scanning electron microscope (SEM) images of nano-rods are shown in Figure 1. Additionally, we have prepared LISs by coating the textured ZnO surfaces with Krytox GPL series oil. As stated in Table 1, three different lubricating oils were employed, including Krytox GPL-101, 105, and 107. Until the surface was totally saturated, oil was poured onto it. In order to remove any remaining oil and create a homogenous layer of oil, the surface was then maintained inclined for 24 hours. The thickness of the lubricants should be comparable to the height of the nano-pillars (6 μm) in order for the oil to fully enter and remain in the area between them. Last but not least, we created four different types of surfaces, including ZnO-textured surfaces devoid of any lubricant film. Water droplets on the prepared slanted samples (10°) were used in the slippery testing.

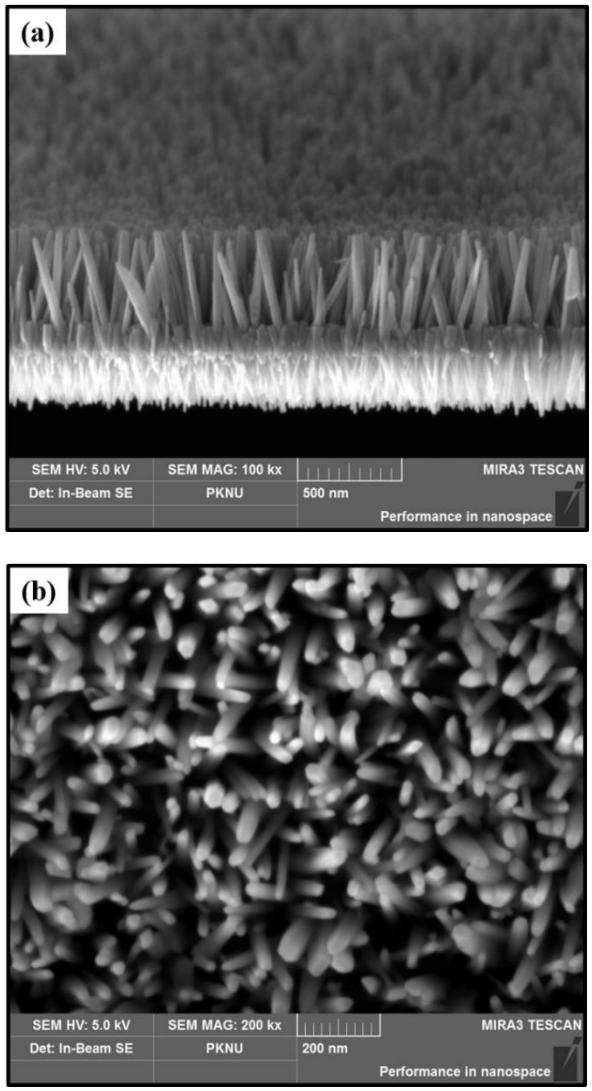

Figure 1. SEM images of ZnO nanorods grown on Zn/Si substrate (a) edge tilt view (b) top view

Table 1. Physical properties of tested lubricant oils

Krytox Oil	*GPL 101*	*GPL 105*	GPL 107
Kinematic Viscosity, (at 20°C) [m^2/s]	17	520	1600
Density (at 0°C) [g/mL]	1.87	1.94	1.95
Surface tension [N/m]	19	20	20

With a droplet height of about 2 cm and a weak falling inertia, water was dropped on the slanted surface. On the dry ZnO-textured surface, a drop first slipped out rapidly and

without any pause. On the other hand, lubricant-infused ZnO-textured surfaces showed a gradual slip motion in the way described below: LIS101 > LIS105 > LIS 107. Lower slip motion is associated with lubricants with greater viscosities.

2.2 Experiments

Figure 2 shows the experimental setup, which includes a syringe pump (Chemyx Fusion 200) that creates droplets of deionized water with a diameter of 2.3 ± 0.05 mm and drops them onto substrates with a ZnO textured surface. The dimensionless Weber number (We) and the Reynolds number (Re) are the main factors affecting impact. *The Weber number*, $We = (\rho D_0 U_0^2)/\sigma$ and the Reynolds number, $Re = \rho D_0 U_0/\mu$, where D_0 is the droplet diameter, ρ is the liquid density, U_0 is the impact velocity, μ is the liquid viscosity, and σ is the liquid-air surface tension between the liquid and the surrounding air. The experimental impact velocity ranges from $0.2 < U_0 < 3.5 \pm 0.01$ m/s, corresponding to $2 < We < 430$ and $560 < Re < 8{,}400$. The high-speed camera revealed the impact velocities, and by reviewing the captured photos, the drop diameter was determined. Prior to testing, the scale of the reference image was used to determine the length of a pixel. The number of droplet-size pixels for each experimental image was multiplied by a scale of measured length. A pixel's length in this study was 15.4 µm/pixel. At least three different runs of each experiment were completed.

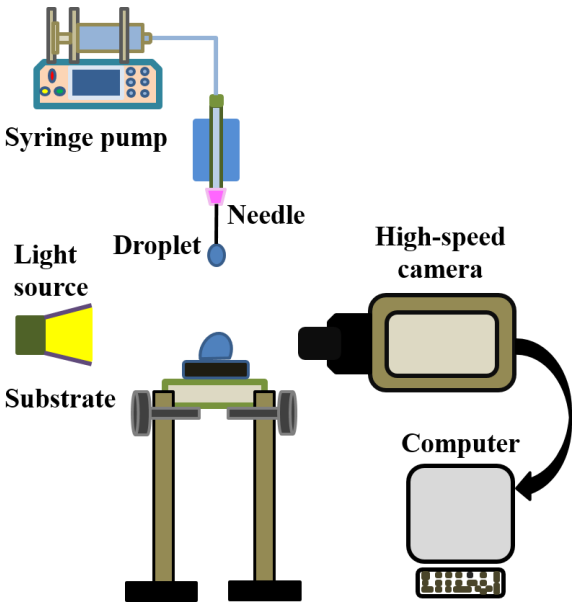

Figure 2. Experimental facility

3. RESULTS AND DISCUSSIONS

3.1 Impact of droplets with and without injected lubricants on a ZnO rough surface

Initially, experiments were performed for various Weber number to investigate the droplet impact dynamics on ZnO textures with and without lubricants. Three types of lubricants used with different viscosities are as shown in the Table 1. The detailed droplet impact event map with increase of We number on ZnO textures with and without lubricants is shown in Figure 3(a). The droplet impact events that were observed matched those described in the literature [21]. The droplet impact process on ZnO surfaces can result in a variety of impact behaviors, including deposition, full rebound, partial rebound, receding breakup, and splash. Using three different lubricants (GPL-101, GPL-105, and GPL-107) on these surfaces, we divided the drop impact behavior into three portions (LIS101, LIS105, and LIS107). This study examines how the physical characteristics of lubricating oils and droplet impact velocity affect the results of drop impacts.

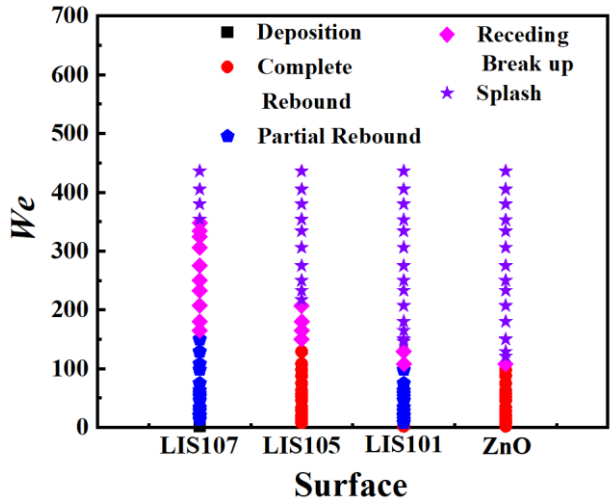

(a)

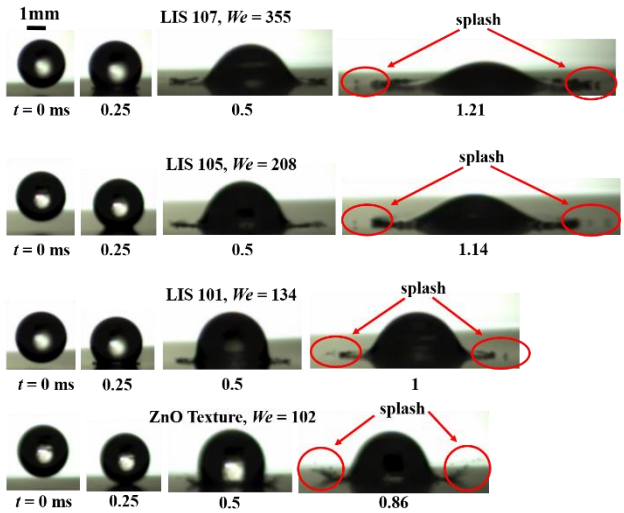

(b)

Figure 3. (a) With and without lubricant (LIS), the Weber number (*We*) of droplets splashing over ZnO-textured surfaces varies over time; (b) Splashing of droplets at different *We* number on dry ZnO textured surfaces and surfaces infused with lubricant

Droplets spread and retracted at low Weber numbers, but as the Weber number increased, the impact behaviors mostly transitioned from "rebound" to "re-ceding breakup" to "splash". In addition to deposition events, the wetting transition also experienced total or partial rebound as a result of variations in water hammer pressure, capillary pressure, and dynamic pressure depending on the degree of liquid penetration in nano-pillars. Also referred to as quick splashing, breaking up during spread occurs along the moving contact line of the liquid lamella. Droplets showed fading breakup after hitting the surface, followed by splashing. Receding breakup predominated at high viscosity lubricant infused ZnO

surface i.e. LIS107, but was suppressed on low viscosity lubricant and dry ZnO textured surfaces. The critical Weber number (Wecr), which changes depending on surface properties, is the minimal Weber number at which splashing occurs under specific circumstances. Through experimental research, we have assessed each critical splashing Weber number (We_{cr}) on LIS and ZnO textured surfaces. The evolution of the droplet impact events with a rise in *We* on ZnO-textured surfaces with and without lubricants is shown in Figure 3(a). The plot unambiguously depicts We_{cr} behavior across all surfaces. It is clear that We_{cr} is on the decline as lubricant viscosity falls. Also worth noting is that the total We_{cr} on the LIS is higher than that of a dry ZnO textured surface. According to Figure 3(b), the droplet splash happens at *We* numbers 355, 208, 134, 102 for LIS107, LIS105, LIS101, and dry ZnO textured surface respectively. Therefore, it's crucial to comprehend how droplet splash happens on LIS and why it takes longer than on a dry ZnO textured surface to happen on LIS.

The splash behavior of droplets on surfaces is influenced by various factors, including surface properties, droplet size, impact velocity, and, importantly, the properties of the surrounding medium, such as the viscosity of the lubricant. Here are the mechanisms by which different viscosities of lubricants affect droplet splash behavior:

Viscous dissipation: The viscosity of the lubricant affects the dissipation of kinetic energy upon droplet impact. Higher viscosity lubricants tend to dissipate more energy, resulting in reduced splashing upon impact. This is because the viscous forces within the lubricant resist the deformation and spreading of the droplet, leading to smoother wetting and reduced ejection of liquid mass.

Capillary forces: Capillary forces, which arise from the surface tension of the droplet, can be affected by the viscosity of the surrounding medium. Higher viscosity lubricants can alter the balance between surface tension and inertial forces during droplet impact, influencing the spreading and retraction dynamics. This can lead to changes in the propensity for splash or splatter behavior, depending on the specific conditions.

Surface wetting and spreading: The viscosity of the lubricant can influence the wetting behavior of the droplet on the surface. Lower viscosity lubricants tend to spread more readily upon impact, leading to thinner wetting films and reduced likelihood of splashing. In contrast, higher viscosity lubricants may resist spreading and maintain thicker wetting films, which can promote splashing under certain conditions, especially at higher impact velocities.

Viscoelastic effects: Some lubricants exhibit viscoelastic behavior, meaning they have both viscous and elastic components in their response to deformation. Viscoelastic effects can influence the dynamic behavior of droplets upon impact, affecting spreading, recoiling, and splashing behavior. The interplay between viscosity, elasticity, and surface tension determines the overall impact dynamics and splash outcomes.

Surface roughness and texture: The presence of surface roughness or texture can interact with the viscosity of the lubricant to modulate droplet impact dynamics. Higher viscosity lubricants may penetrate into surface features more slowly, leading to altered spreading and splashing behavior compared to lower viscosity lubricants. Additionally, the viscoelastic properties of the lubricant can affect its interaction with surface asperities, influencing droplet wetting and splashing.

The viscosity of lubricants can significantly impact droplet splash behavior through its influence on energy dissipation, capillary forces, wetting dynamics, viscoelastic effects, and interactions with surface roughness. Understanding these mechanisms is crucial for controlling splashing phenomena in various applications, such as lubricated systems, coating processes, and droplet-based technologies.

3.2 The function of adhesive force in droplet splash delay on ZnO textures impregnated with lubricant

Existing studies looked on sticky super-hydrophobic surfaces' anti-splashing characteristics [34]. For the droplet splash event, zinc oxide (ZnO) nanowires and anodic aluminum oxide (AAO) with sealed air pockets were compared. The results of the aforementioned study showed that the high adhesion force properties of the superhydrophobic AAO surface effectively limit droplet splashing. In contrast, because there was an air layer between the impacting water drop and the solid surface, the ZnO surface induced droplet splashing. Based on the aforementioned study, we considered the adhesive force as an important parameter that can delay droplet splash on lubricant infused ZnO textured surfaces. Therefore, we measured the adhesive (surface) force by considering surface tension and meniscus length wherein the force acts on the relative surface during detachment from the droplet. Thus, we initially placed a droplet of large size with a volume of approximately 60 µl on the surface and then used the DuNouytensiometer to measure interfacial tension as shown in Figure 4(a). In the experiment, we obtained the length along which force acts (L). We then obtained the adhesive (surface) force by using the following expression:

$$\sigma = \frac{F_a}{L}$$

where, σ denotes the surface tension, F_a denotes the adhesive force and L denotes the length where the force acts as shown in Figure 4(a). Thus, adhesive force values are measured on all surfaces in our study as shown in Figure 4(b). Additionally, ZnO textures infused with lubricant GPL107 (LIS107) showed the strongest adhesive force, followed by dry ZnO structured surfaces, LIS105, and LIS101. Based on this analysis, we hypothesise that the high adhesive force on LIS 107 is responsible for the higher values of We_{cr}, and the very low adhesive force on the dry ZnO textured surface, which results in earlier splashing than on LIS surfaces, is the cause of the lowest value of We_{cr}.

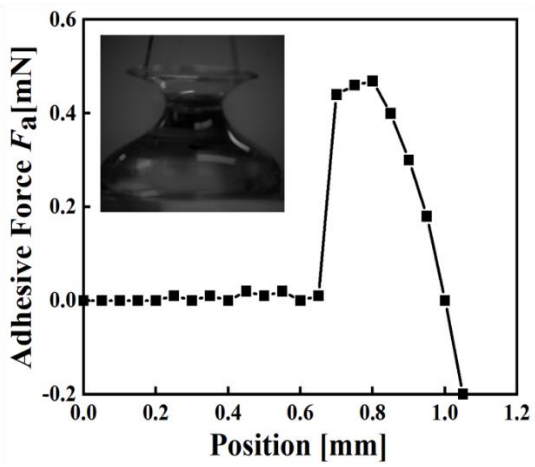

(a)

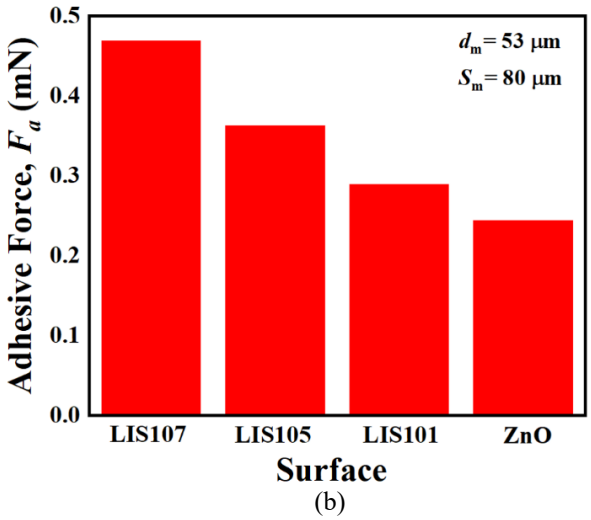

(b)

Figure 4. (a) Determining the adhesive force and the length of the interfacial tension where the force acts; (b) Adhesive force comparison across all surface types

4. CONCLUSION

In order to evaluate the impact of adhesion on droplet splashing behaviors, two distinct super-hydrophobic surfaces dry nano-structured surfaces and lubricant infused nano-structured surfaces—are created. As a result of their surface properties, lubricant-infused nano-structured surfaces adhered to them better than dry nano-structured surfaces. Because there was an air layer between the impacting water drop and the solid surface, splashing was encouraged when the droplet hit the dry nano-structured surface. On lubricant-infused nano-structured surfaces, however, droplet splashing was not seen under the same circumstances because stronger adhesion prevented Plateau-Rayleigh instability, which caused the lifting of the spreading front of the water droplets.

ACKNOWLEDGMENT

This work was supported by National Research Foundation of Korea (NRF) and Pukyong National University, South Korea.

REFERENCES

[1] Damak, M., Hyder, M.N., Varanasi, K.K. (2016). Enhancing droplet deposition through in-situ precipitation. Nature Communications, 7: 12560. https://doi.org/10.1038/ncomms12560

[2] Song, M., Ju, J., Luo, S., Han, Y., Dong, Z., Wang, Y., Gu, Z., Zhang, L., Hao, R., Jiang, L. (2017). Controlling liquid splash on superhydrophobic surfaces by a vesicle surfactant. Science Advances, 3(3): e1602188. https://doi.org/10.1126/sciadv.1602188

[3] Bhushan, B., Jung, Y.C., Koch, K. (2009). Self-cleaning efficiency of artificial superhydrophobic surfaces. Langmuir, 25(5): 3240-3248. https://doi.org/10.1021/la803860d

[4] Feng, X.J., Jiang, L. (2006). Design and creation of superwetting/antiwetting surfaces. Advanced Materials, 18(23): 3063-3078. https://doi.org/10.1002/adma.200501961

[5] Darmanin, T., Guittard, F. (2014). Recent advances in the potential applications of bioinspired superhydrophobic materials. Journal of Materials Chemistry A, 2(39): 16319-16359. https://doi.org/10.1039/C4TA02071E

[6] Tian, X., Verho, T., Ras, R.H. (2016). Surface wear. Moving superhydrophobic surfaces toward real-world applications. Science, 352: 142-143. https://doi.org/10.1126/science.aaf2073

[7] Simpson, J.T., Hunter, S.R., Aytug, T. (2015). Superhydrophobic materials and coatings: A review. Reports on Progress in Physics, 78(8): 086501. https://doi.org/10.1088/0034-4885/78/8/086501

[8] Jeevahan, J., Chandrasekaran, M., Britto Joseph, G., Durairaj, R.B., Mageshwaran, G. (2018). Superhydrophobic surfaces: A review on fundamentals, applications, and challenges. Journal of Coatings Technology and Research, 15: 231-250. https://doi.org/10.1007/s11998-017-0011-x

[9] Rothstein, J.P. (2010). Slip on superhydrophobic surfaces. Annual Review of Fluid Mechanics, 42: 89-109. https://doi/10.1146/annurev-fluid-121108-145558

[10] Quere, D. (2005). Non-sticking drops. Reports on Progress in Physics, 68: 2495-2532. https://doi/10.1088/0034-4885/68/11/R01

[11] Zhou, S., Jiang, L., Dong, Z. (2020). Bioinspired surface with superwettability for controllable liquid dynamics. Advanced Materials Interfaces, 8(2): 2000824. https://doi.org/10.1002/admi.202000824

[12] Zhan, S.S., Pan, Y., Gao, Z.F., Lou, X.D., Xia, F. (2018). Biological and chemical sensing applications based on special wettable surfaces. TrAC Trends in Analytical Chemistry, 108: 183-194. https://doi.org/10.1016/j.trac.2018.09.001

[13] Ban, G.H., Lee, J., Choi, C.H., Li, Y., Jun, S. (2017). Nano-patterned aluminum surface with oil-impregnation for improved antibacterial performance. LWT, 84: 359-363. https://doi.org/10.1016/j.lwt.2017.05.061

[14] Hong, X., Gao, X., Jiang, L. (2007). Application of superhydrophobic surface with high adhesive force in no lost transport of superparamagnetic microdroplet. Journal of the American Chemical Society, 129(6): 1478-1479. https://doi.org/10.1021/ja065537c

[15] Park, S.G., Moon, J.H., Lee, S.K., Shim, J., Yang, S.M. (2010). Bioinspired holographically featured superhydrophobic and supersticky nanostructured materials. Langmuir, 26(3): 1468-1472. https://doi.org/10.1021/la9035826

[16] Zhu, H., Guo, Z., Liu, W. (2014). Adhesion behaviors on superhydrophobic surfaces. Chemical Communications, 50(30): 3900-3913. https://doi.org/10.1039/c3cc47818a

[17] Wang, S., Jiang, L. (2007). Definition of superhydrophobic states. Advanced Materials, 19(21): 3423-3424. https://doi.org/10.1002/adma.200700934

[18] Antonini, C., Amirfazli, A., Marengo, M. (2012). Drop impact and wettability: From hydrophilic to superhydrophobic surfaces. Physics of Fluids, 24: 102104. 102104. https://doi.org/10.1063/1.4757122

[19] Quetzeri-Santiago, M.A., Castrejon-Pita, A.A., Castrejon-Pita, J.R. (2019). The effect of surface roughness on the contact line and splashing dynamics of impacting droplets. Scientific Reports, 9: 15030. https://doi.org/10.1038/s41598-019-51490-5

[20] Hao, J.G. (2017). Effect of surface roughness on droplet splashing. Physics of Fluids, 29: 122105. https://doi.org/10.1063/1.5005990
[21] Yarin, A.L. (2006). Drop impact dynamics: Splashing, spreading, receding, bouncing. Annual Review of Fluid Mechanics, 38: 159-192. https://doi.org/10.1146/annurev.fluid.38.050304.092144
[22] Koch, K., Grichnik, R. (2016). Influence of surface structure and chemistry on water droplet splashing. Philosophical Transactions of the Royal Society A, 374(2073): 20160183. https://doi.org/10.1098/rsta.2016.0183
[23] Quintero, E.S., Riboux, G., Gordillo, J.M. (2019). Splashing of droplets impacting superhydrophobic substrates. Journal of Fluid Mechanics, 870: 175-188. https://doi.org/10.1017/jfm.2019.258
[24] Liu, Y., Tan, P., Xu, L. (2015). Kelvin-Helmholtz instability in an ultrathin air film causes drop splashing on smooth surfaces. Proceedings of the National Academy of Sciences of the United States of America, 112(11): 3280-3284. https://doi.org/10.1073/pnas.1417718112
[25] Huang, X., Wan, K.T., Taslim, M.E. (2018). Axisymmetric rim instability of water droplet impact on a super-hydrophobic surface. Physics of Fluids, 30: 094101. https://doi.org/10.1063/1.5039558
[26] Sapkal, N.P., Park, S.C., Lee, Y.W., Yu, D.I. (2021). Experimental study of droplet splashing phenomena on hydrophobic micro-and micro/nano-textured surfaces. Journal of Mechanical Science and Technology, 35: 5061-5070. https://doi.org/10.1007/s12206-021-1023-0
[27] Sapkal, N.P., Lee, Y.W., Park, S.C., Yu, D.I. (2023). Droplet splashing and retraction dynamics on micro/nano-textured surfaces with or without infused lubricants: An experimental approach. Journal of Mechanical Science and Technology, 37: 3525-3533. https://doi.org/10.1007/s12206-023-0618-z
[28] Jung, Y.C., Bhushan, B. (2009). Dynamic effects induced transition of droplets on biomimetic superhydrophobic surfaces. Langmuir, 25(16): 9208-9218. https://doi.org/10.1021/la900761u
[29] Wong, T.S., Kang, S.H., Tang, S.K.Y., Smythe, E.J., Hatton, B.D., Grinthal, A., Aizenberg, J. (2011). Bioinspired self-repairing slippery surfaces with pressure-stable omniphobicity. Nature, 477: 443-447. https://doi.org/10.1038/nature10447
[30] Lafuma, A., Quere, D. (2011). Slippery pre-suffused surfaces. Europhysics Letters, 96(5): 56001. https://doi.org/10.1209/0295-5075/96/56001
[31] Chen, L., Auernhammer, G.K., Bonaccurso, E. (2011). Short time wetting dynamics on soft surfaces. Soft Matter, 7: 9084-9089. https://doi.org/10.1039/C1SM05967J
[32] Chen, L., Bonaccurson, E., Shanahan, M.E.R. (2013). Inertial to viscoelastic transition in early drop spreading on soft surfaces. Langmuir, 29(6): 1893-1898. https://doi.org/10.1021/la3046862
[33] Sapkal, N.P. (2021). Experimental investigations on the ignition delay time of freely falling liquid fuel droplets. International Journal of Heat and Technology, 39(3): 987-991. https://doi.org/10.18280/ijht.390336
[34] Kim, W., Eun, J., Jeon, S. (2021). Anti-splashing properties of sticky superhydrophobic surfaces. Applied Surface Science, 542: 148617. https://doi.org/10.1016/j.apsusc.2020.148617

NOMENCLATURE

We_{cr}	Critical Weber number
σ	Surface Tension
F_a	Adhesive force
L	Length